Proceedings of 20th International Congress on Acoustics, ICA 2010

23-27 August 2010, Sydney, Australia

Electro-acoustic transducers with cellular polymer electrets

Yoshinobu Yasuno, Hidekazu Kodama, Munehiro Date and Eiichi Fukada

Kobayasi Institute of Physical Research, 3-20-41, Higashi-motomachi, Kokubunji, Tokyo 185-0022, Japan

PACS: 43.38.BS

ABSTRACT

Electroacoustic transducers utilizing the piezoelectric d_{33} coefficient of cellular polypropylene electrets generally employ two processes, corona charging and expansion of the voids to increase the piezoelectric constant. However, earlier works noted instability of the transducer performance due to changes in the material structure because the second process applied to expand the voids and required a stacked structure. Additionally, the transducers should be driven by a few hundreds of volts to generate a sufficient sound-pressure level. The effective frequency band became narrower with the increased number of stacked sheets. Therefore, consumer applications were limited.

This paper describes ultrasonic transducers of porous polypropylene electrets that exhibit 250 to 350 pC/N of d_{33} without applying second process. First, the piezoelectric constant of the sample was evaluated by the dielectric-resonance method. The change of piezoelectric coefficient was studied for utilizing stable sample. Next, in order to realize a robust transducer, a low-voltage drive should be possible for transmitters, and flat frequency characteristics with high sensitivity for receivers should be realized in a package with simple structure. Transmitters and receivers are designed experimentally. The material that stabilizes the piezoelectric d_{33}-coefficient of 250 to 350 pC/N is estimated to determine the optimal frequency band and driving method. This paper will also report temperature stability as utilization research and application in an airborne ultrasonic range.

INTRODUCTION

In recent years, electrets of cellular structured polymers have received attention as a new piezoelectric material with a high piezoelectric d_{33} coefficient over 100 pC/N. In particular, research on porous polypropylene film has been carried out for both improvement of physical characteristics and application [1]-[5]. The acoustic impedance is low, and some research has verified the validity in the ultrasonic range in air, but high-voltage operation is required and is not practical [6]. This study evaluated piezoelectric coefficients of cellular polypropylene by means of dielectric spectroscopy. Next, a transmitter-and-receiver device was developed as a simple experimental structure in the stable domain of a piezoelectric coefficient to estimate performance and temperature stability in a low-voltage drive. As an application, short distance domain measurement by a combined transmitter and receiver combination is reported.

SAMPLE

A porous PP sheet (provided by YUPO Corporation) was used as a sample. This sample's thickness was 85 μm, and its density was 490 kg/m^3. Aluminium electrodes were deposited on both surfaces of the sample. A corona discharge was applied to one side of the sample, with -10 kV in a grid electrode and -18 kV in a needle electrode. The other side electrode was connected to a ground terminal while charging. Both electrodes were shorted after the discharge.

Dielectric Resonance to Measure Piezoelectric Properties

Figure 1 depicts the frequency spectra of the real part $\varepsilon'/\varepsilon_0$ and imaginary part $\varepsilon''/\varepsilon_0$ of the relative complex permittivity measured before charging, just after charging, a day after charging, and 6 days after charging. These frequency characteristics were caused by the thickness mode of the piezoelectric response [7]. The permittivity in fixed condition ε^S, the elastic constant c_{33}, the piezoelectric constants e_{33} and d_{33} (= e_{33}/c_{33}), and the electromechanical coupling factor k_t (= $(e_{33}^2/c_{33}\varepsilon^S)^{1/2}$) were obtained by fitting the experiment results with the following equation:

$$\varepsilon^* = \varepsilon^S / [1 - k_t^2 \{\tan(\omega h/2v)\}/(\omega h/2v)], \qquad (1)$$

where ε^* is complex permittivity, ω is angular frequency, and h is the thickness of the sample. Here, v is the acoustic velocity defined as $v^2 = c_{33}/\rho$, where ρ is density.

In Fig. 2, $\varepsilon^S/\varepsilon_0$, c_{33}, e_{33}, d_{33}, and k_t were plotted against storage time in hours. For the sample just after charging, $\varepsilon^S/\varepsilon_0$ = 1.45, k_t = 0.094, c_{33} = 0.95 MPa, e_{33} = 330 μC/m^2, and d_{33} = 350 pC/N. One day after charging, $\varepsilon^S/\varepsilon_0$ increased to 1.50, and c_{33} increased to 1.0 MPa. However, k_t decreased to 0.064, e_{33} decreased to 231 μC/m^2, and d_{33} decreased to 233 pC/N. Thereafter, they were almost constant.

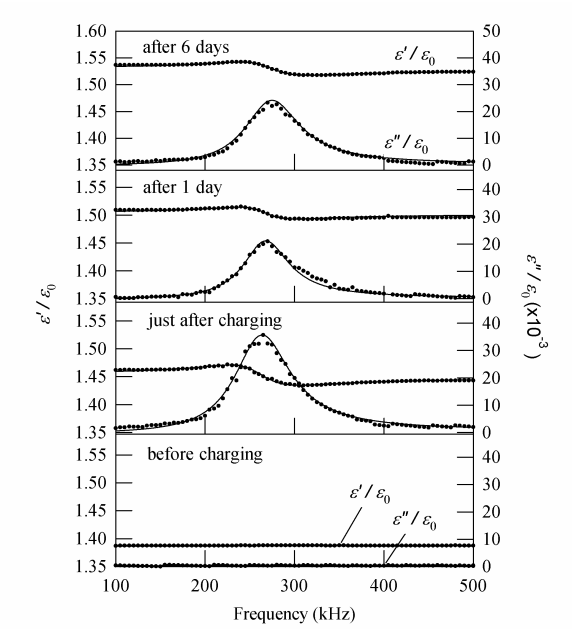

Fig. 1. Frequency spectra of the real part $\varepsilon'/\varepsilon_0$ and imaginary part $\varepsilon''/\varepsilon_0$ of relative permittivity of the samples before charging, just after charging, 1 day after charging, and 6 days after charging

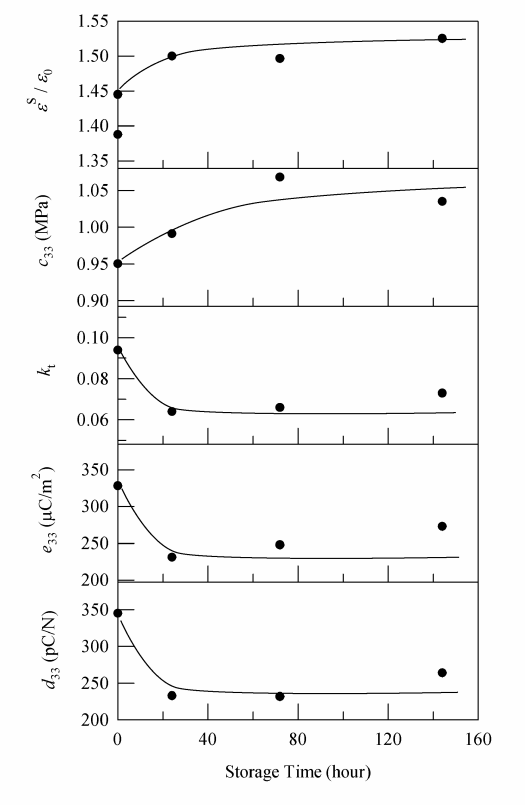

Fig. 2. Plots of permittivity $\varepsilon^S/\varepsilon_0$, electromechanical coupling coefficient k_t, elastic constant c_{33}, piezoelectric constant e_{33}, and piezoelectric constant d_{33} against storage time

EXPERIMENTAL MODEL OF THE ULTRASONIC TRANSMITTER

The ultrasonic transducer was developed as an experiment, using the same material as for the piezoelectric d_{33} coefficient described above [8].

Material specification and structure of the Ultrasonic transducer

The structure of the transmitter (Tx) depicted in Fig. 3, and the main specifications for the porous polypropylene experiment are presented in Table 1. The drive voltage is directly impressed to both sides of the electrode of the Tx; a receiver (Rx) is operated through an impedance converter (FET), and metal shielding is applied.

Table 1. Specifications of specimens.

Thickness [μm]	72	*Piezoelectric coefficient* d_{33} [pC/N]	250
Basis weight [g/m^2]	34.9	*Electromechanical Coupling coefficient* k_t	1.44
Void content [%]	55		

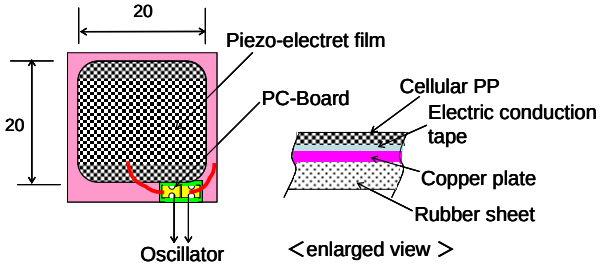

Fig. 3. Structure of the Experimental Transmitter.

Performance of the Ultrasonic Transmitter

Conventionally, an ultrasonic Tx for the airborne ultrasonic range is a resonated adapting PZT, and the resonance frequency is 40 kHz. With standard performance, the output sound pressure of 100 dB/10Vp-p at a distance of 300 mm is used for the application apparatus for which the distance from the sound source is assumed to be 0.2 to 5 m. And the following were evaluated:

1) Frequency characteristics of output sound pressure level (Fig. 4)

2) Input-output response of Tx (Fig. 5)

3) Sound pressure level vs. distance (Fig. 6).

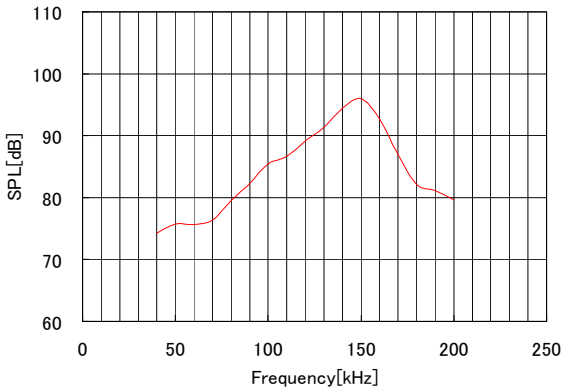

Fig. 4. Sound pressure level of the Cellular PP Transmitter.

(r=300 mm, Vin=20 $V_{p\text{-}p}$)

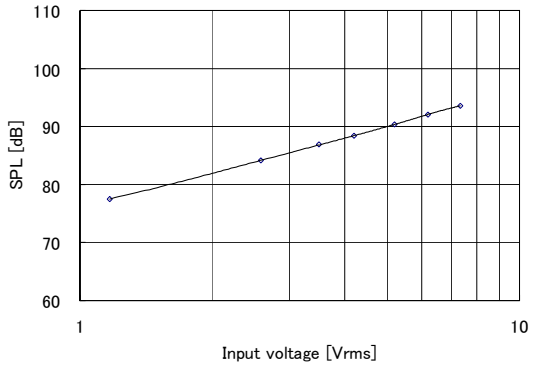

Fig. 5. Sound Pressure level vs. Input voltage. (r=300 mm, f=145 kHz)

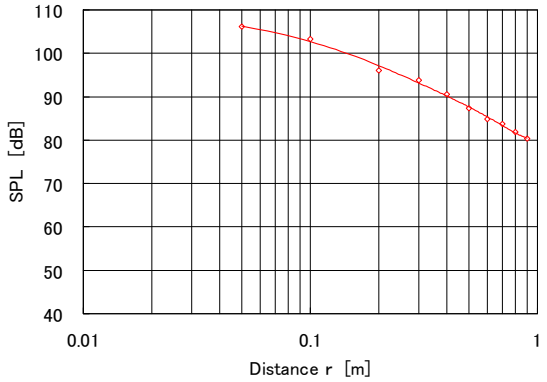

Fig. 6. Sound pressure level vs. Distance from the Transmitter. (Vin=20 $V_{p\text{-}p}$, f=145 kHz)

Tx-Rx Mutual Characteristics

Both a Tx and a Rx were used in an experiment with porous polypropylene film. An ultrasonic signal was sent from the Tx, and the Rx received it at a distance of 300 mm. The response level of the Rx is the open-circuit output voltage of the source-grounded circuit in J-FET. The response level is defined as the ratio of Rx output voltage to Tx input voltage (Fig. 7). As for the peak of sensitivity, the response level of -56 dB is determined from a receiving output of 11 mVrms and a transmitting input of 7.1Vrms at 150 kHz. Since the response levels of a commercial PZT device are -60 to -70 dB at 300 mm and 200 kHz, a more sensitive transducer was realized.

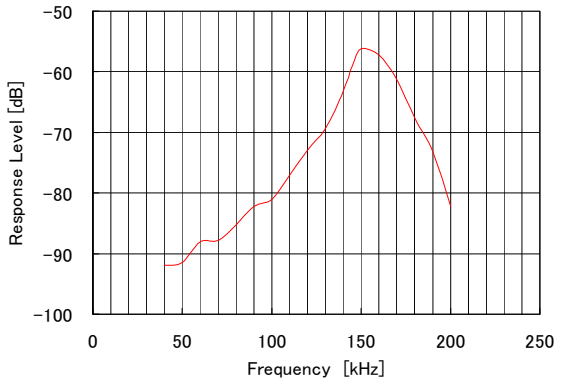

Fig. 7. Cellular PP Tx-Rx Mutual Characteristics(r=300 mm) ※Response level=20*Log(Rx Output Voltage/ Tx Input Voltage)

MEASUREMENT

Short Distance Domain Measurement

An ultrasonic burst signal that input three waves into the TTL circuit was generated from the Tx through Analog SW, and the Rx received the signal. The time required to travel from the Tx to the Rx was measured, and the distance was determined from the acoustic velocity. Figure 8 depicts an example of the result. Here, the propagation time from the Tx to the Rx was 630 μsec, and the distance was determined to be 0.218 m from the sound velocity of 346.8 m/sec at 25 ℃. This value was in agreement with the actual measurement of 0.217 m. Furthermore, the distance between the actual Tx and Rx was changed, and the distance calculated from the propagation delay time is presented in Fig. 9. The obtained data was in good agreement with the ideal value (red dotted line).

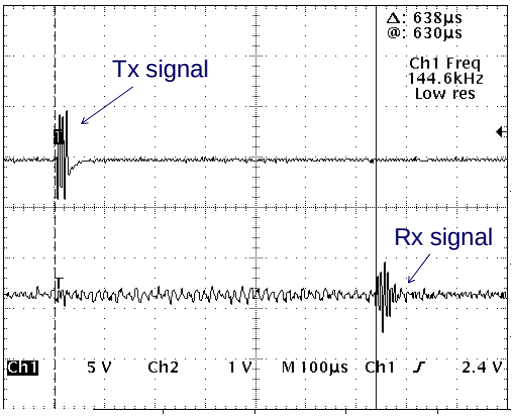

Fig. 8. Example of short range measurement.

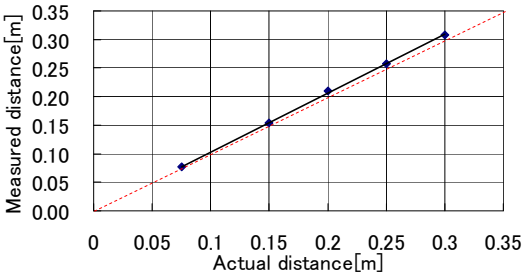

Fig. 9. Actual distance vs. measured distance.

Operation of the Tx-Rx Combined Type

In the previous section, Tx and Rx operation was checked using separate devices. The operation circuit of Tx and Rx that shared a device was then investigated as an experiment. A brass board (100 mm x 1 mm) was placed as a target, and a range-finding experiment was conducted. Figure 10 depicts this operation circuit, where R1 is 100 kΩ, R2 is 39 kΩ, and R3 is 2.2 kΩ. Since the capacity of a transducer is 100 pF, R1 is set so that it may become a time constant shorter than the delay time for measuring distance. As R2 determines the high cut off frequency of the Rx, it is set so that the required frequency range can be secured. Figure 11 depicts an example of the measurement results. The 20 Vp-p ultrasonic signal of 145 kHz is sent to the target. A delay time of 590 μsec sec was measured at 200 mm in both directions, and the calculated values from the acoustic velocity for that time and survey were in good agreement.

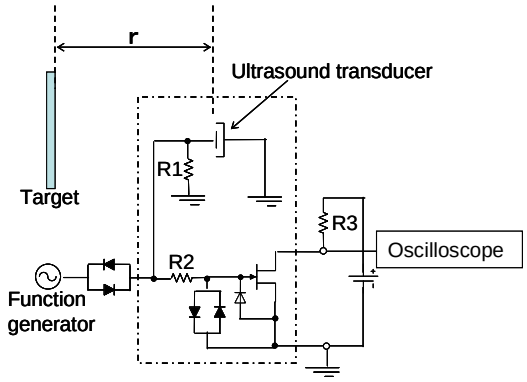

Fig. 10. Tx-Rx combined operation circuit.

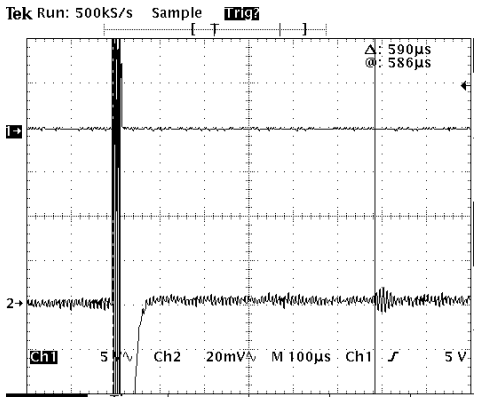

Fig. 11. Distance measurement by Tx-Rx combination.

Temperature Characteristics of the Ultrasonic Transmitter

The Tx output sound pressure level with an input voltage of 20 Vp-p and a frequency of 40 kHz to 200 kHz was measured. Distance r from Tx to the microphone was set to 50mm, measuring 40 to 80 kHz with the 1/4in microphone, and 80 to 200 kHz with the 1/8in microphone (Fig. 12). The sound pressure level went up with a rise in heat, and the resonating point peak changed from 170 kHz to 125 kHz. This change of resonance could be presumed from the change of thickness of the sample. The output becomes unstable at high temperatures; thus, observation was not possible at temperatures above 60 °C.

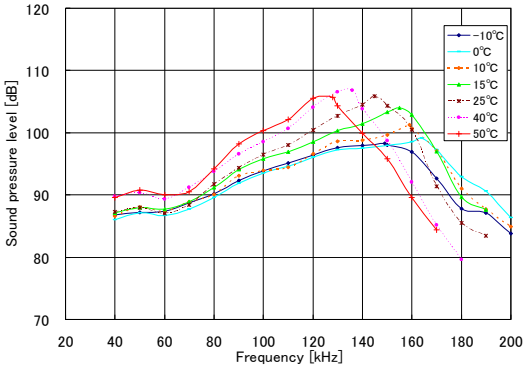

Fig. 12. Temperature characteristics of the sound pressure level of Tx. (r=50 mm, V_{in}=20 V_{p-p})

DISCUSSION

Short Distance Domain Measurement

Non-contact and short-range detection has many uses. However, in order to realize stable measurement with a simple structure, a common device must be used. Experimentally, since the amplitude of the burst signal differed greatly from the amplitude of the reflected signal when a Tx-Rx combined device was used, detection was attempted in a basic circuit combined with an impedance converter of the receiver (Fig. 10). Improvement is required for the optimal circuit of operation to demonstrate a device's performance.

Attribution Analysis of Temperature Characteristics Change

The common structure portion of the Tx and the receiver is analyzed from the transmitter characteristic change. The resonance frequency of the transmitter decreases with increasing heat. A structural model of porous polymer is considered (Fig. 13). Assuming that change of resonance frequency by temperature has resulted from the dimensional change of the volume of air layer, the volume V of ideal gas is proportional to the absolute temperature at the condition of pressure regularity, according to Charles's Law.

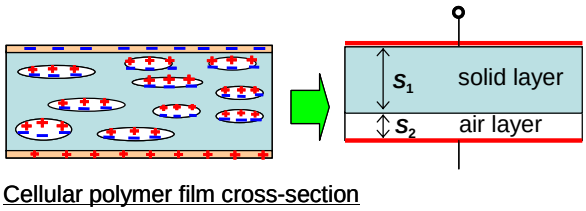

Fig. 13. Electro-mechanical simplified model.

For example, the change in volume for temperatures of 10 °C and 50 °C is calculated as follows.

$$\frac{V_{10°c}}{T_{10°c}} = \frac{V_{50°c}}{T_{50°c}} \qquad (1)$$

Therefore, the volume ratio of the air layer is

$$\frac{V_{50°c}}{V_{10°c}} = \frac{273+50}{273+10} \approx 1.14 . \qquad (2)$$

However, the resonance frequency is

$$f_0 = \frac{1}{2\pi S}\sqrt{\frac{E}{\rho}} , \qquad (3),$$

where E is Young's modulus, ρ is density, and S is thickness.

Resonance frequency increases 0.81 times at 50 °C, compared with 10 °C, and the thickness of the air layer changes by 1.24 times (Eq. (3)) in the domain in which Young's modulus and others remain constant. The thickness of the air layer increases compared with the volume ratio of Eq. (2), and a horizontal cross section is assumed to become 0.91 times smaller.

As mentioned above, the change of air layer is considered due to the temperature change of a piezoelectric transducer. The temperature change of the piezoelectric transducer is a key factor in controlling the space. However, as overall sensitivity decreases at temperatures below 0 °C and the peak of resonance frequency cannot be judged, it is necessary to consider other factors.

CONCLUSION

1) The stability of a porous polypropylene film was defined by measuring the time-dependent change of piezoelectric coefficients.

2) As an experiment, the ultrasonic transducer was evaluated for frequency, input and output, and decay-by-distance characteristics. The sound pressure level reached 96 dB/20 Vp-p at a distance of 300 mm and a frequency of 150 kHz.

3) In Tx and Rx mutual characteristic, performance at 150 kHz exceeded the overall characteristics of a 200 kHz range PZT device.

4) The possibility of range-finding from propagation delay time was confirmed in the short-distance domain.

5) The dimensional change of the air layer with temperature is a key factor in the structure of the Tx and Rx common portion, and compensation for this change should be considered necessary for a robust transducer.

ACKNOWLEDGEMENT

The authors would like to acknowledge the kind help of Prof. G. M. Sessler and Dr. M. Paajanen at the initial stage of the study.

REFERENCES

[1] J. Lekkala and M. Paayanen, “EMFi - New Electret Material for Sensor and Actuators,” Proc. 10th International Symp. Electrets, (1999).

[2] G. S. Neugschwandtner, R. Schwodiauer, M. Vieytes, S. Bauer-Gogonea, S. Bauer, J. Hillenbrand, R. Kressmann, G. M. Sessler, M. Paajanen, and J. Lekkala, “Large and broadband pieezoelectricity in smart polymer-foam space-charge electrets,” Appl. Phys. Lett., vol. 77, no. 23, pp. 3827-3829,(2000).

[3] J. Hillenbrand and G. M. Sessler, “Piezoelectricity in Cellular Electret Films,” IEEE Trans. Dielectr. Electr. Insul., vol. 7, no. 4, pp. 537 - 542,(2000).

[4] M. Paajanen, J. Lekkala and H. Valimaki, “Electromechanical Modeling and Properties of the Electret Film EMFI,” IEEE Trans. Dielectr. Electr. Insul., vol. 8, no. 4, pp. 629 - 636, (2001).

[5] X. Zhang, G. M. Sessler, and J. Hillenbrand, “Improvement of Piezoelectric Coefficient of Cellular Polypropylene Films by Repeated Expansions,” J. Electrostatics, vol. 62, pp. 94-100,(2007).

[6] L.Reinhard, et al., 19th ICA, Madrid, (2007).

[7] Axel Mellinger, “Dielectric Resonance Spectroscopy: a Versatile Tool in the Quest for Better Piezoelectric Polymers”, IEEE Trans. Dielectr. Electr. Insul., vol. 10, no. 5, pp. 842–861, (2003).

[8] Hidekazu Kodama, Yoshinobu Yasuno, Munehiro Date, and Eiichi Fukada, “A Study of Time Stability of Piezoelectricity in Porous Polypropylene Electrets”, 2009 IEEE International Ultrasonics Symposium , Roma, Sep. (2009).